0026-895X/09/7603-560–568$20.00
MOLECULAR PHARMACOLOGY
Copyright © 2009 The American Society for Pharmacology and Experimental Therapeutics
Mol Pharmacol 76:560–568, 2009

Vol. 76, No. 3
57265/3503546
Printed in U.S.A.

The Na^+/Ca^{2+} Exchange Inhibitor 2-(2-(4-(4-Nitrobenzyloxy)phenyl)ethyl)isothiourea Methanesulfonate (KB-R7943) Also Blocks Ryanodine Receptors Type 1 (RyR1) and Type 2 (RyR2) Channels

Genaro Barrientos, Diptiman D. Bose, Wei Feng, Isela Padilla, and Isaac N. Pessah

Department of Molecular Biosciences, School of Veterinary Medicine, University of California, Davis, California

Received April 22, 2009; accepted June 9, 2009

ABSTRACT

Na^+/Ca^{2+} exchanger (NCX) is a plasma membrane transporter that moves Ca^{2+} in or out of the cell, depending on membrane potential and transmembrane ion gradients. NCX is the main pathway for Ca^{2+} extrusion from excitable cells. NCX inhibitors can ameliorate cardiac ischemia-reperfusion injury and promote high-frequency fatigue of skeletal muscle, purportedly by inhibiting the Ca^{2+} inward mode of NCX. Here we tested two known NCX inhibitors, 2-(2-(4-(4-nitrobenzyloxy)phenyl)ethyl)-isothiourea methanesulfonate (KB-R7943) and the structurally related 2-[[4-[(4-Nitrophenyl)methoxy]phenyl]methyl]-4-thiazoli dinecarboxylic acid ethyl ester (SN-6), for their influence on electrically or caffeine-evoked Ca^{2+} transients in adult dissociated flexor digitorum brevis (FDB) skeletal muscle fibers and human embryonic kidney (HEK) 293 cells that have stable expression of type 1 ryanodine receptor (RyR1). KB-R7943 ($\leq$10 μM) reversibly attenuates electrically evoked Ca^{2+} transients in FDB and caffeine-induced Ca^{2+} release in HEK 293, whereas the structurally related NCX inhibitor SN-6 does not, suggesting that KB-R7943 directly inhibits RyR1. In support of this interpretation, KB-R7943 inhibits high-affinity binding of [^{3}H]ryanodine to RyR1 (IC_{50} = 5.1 $\pm$ 0.9 μM) and the cardiac isoform RyR2 (IC_{50} = 13.4 $\pm$ 1.8 μM). KB-R7943 interfered with the gating of reconstituted RyR1 and RyR2 channels, reducing open probability (P_o), shortening mean open time, and prolonging mean closed time. KB-R7943 was more effective at blocking RyR1 with cytoplasmic conditions favoring high P_o compared with those favoring low P_o. SN-6 has negligible activity toward altering [^{3}H]ryanodine binding of RyR1 and RyR2. Our results identify that KB-R7943 is a reversible, activity-dependent blocker of the two most broadly expressed RyR channel isoforms and contributes to its pharmacological and therapeutic activities.

The Na^+/Ca^{2+} exchanger (NCX) is a Ca^{2+} extruder that is powered by the energy of the Na^+ gradient across the cell membrane, which is ultimately derived from the Na^+/K^+ ATPase activity. Depending on ionic concentration and membrane potential, NCX can mediate Ca^{2+} efflux (forward mode) or Ca^{2+} influx (reverse mode) (Blaustein and Lederer, 1999). In cardiac muscle under normal physiological conditions, NCX is mainly responsible for Ca^{2+} extrusion from the myocyte. The influx component may occur either during the initial phase of the action potential or under pathological conditions such as ischemia and reperfusion injury (Lytton, 2007). NCX also plays a significant role in maintaining skeletal muscle Ca^{2+} homeostasis (Fraysse et al., 2001; Sokolow et al., 2004). Three NCX isoforms have been identified, and two of these, NCX1 and NCX3, are expressed in skeletal muscle (Fraysse et al., 2001), and their activity contributes to fatigue resistance (Sokolow et al., 2004; Germinario et al., 2008). Reverse operation of NCX has also been proposed as a contributor to neuronal Ca^{2+} overload during anoxia and ischemia (Stys et al., 1992).

KB-R7943 is an inhibitor that is frequently used as an experimental tool to assess the contribution of all three members of the NCX family (NCX1, NCX2, and NCX3) to physiological and pathophysiological processes. Concentrations ranging from 1 to 5 μM produce a half-maximal block (IC_{50}) of the NCX reverse mode (inhibition of Ca^{2+} entry), and

This work was supported by the National Institutes of Health National Institute of Arthritis and Musculoskeletal and Skin Disease [Grants 1R01-AR43140, 1P01-AR52354].

Article, publication date, and citation information can be found at http://molpharm.aspetjournals.org.

doi:10.1124/mol.109.057265.

ABBREVIATIONS: NCX, Na^+/Ca^{2+} exchanger; FDB, flexor digitorum brevis; RyR, ryanodine receptor; ECC, excitation-contraction coupling; KB-R7943, 2-(2-(4-(4-nitrobenzyloxy)phenyl)ethyl)isothiourea methanesulfonate; SN-6, 2-[[4-[(4-nitrophenyl)methoxy]phenyl]methyl]-4-thiazoli dinecarboxylic acid ethyl ester; HEK, human embryonic kidney; BLM, bilayer lipid membrane; Ry, ryanodine; FDB, flexor digitorum brevis; wt, wild type.

inhibition is not selective among the three NCX isoforms (Iwamoto, 2004). KB-R7943 has been used to selectively inhibit the reverse mode of NCX to understand its contribution to cardiac ischemia and injury (Schröder et al., 1999; Seki et al., 2002; Amran et al., 2003; Baczkó et al., 2003; Iwamoto, 2004; Stys, 2004; Dietz et al., 2007; MacDonald and Howlett, 2008; O'Rourke, 2008). However, besides its effect on NCX, KB-R7943 also has off-target effects, including binding to the norepinephrine transporter, ($IC_{50} < 3$ μM) (Matsuda et al., 2001) and block of Ba^{2+} currents through $Ca_v1.2$ with inhibitory constants similar to those needed to inhibit NCX ($IC_{50} = 6.8$ μM) (Ouardouz et al., 2005). KB-R7943 also inhibits currents through $\alpha3\beta4$ and $\alpha7$ nicotinic acetylcholine receptors ($IC_{50} = 0.4$ μM) (Pintado et al., 2000) and inhibits members of transient receptor potential channels with an IC_{50} ranging from 0.5 to 1.4 μM (Kraft, 2007). More recently, KB-R7943 has been also shown to inhibit the mitochondrial Ca^{2+} uniporter ($IC_{50} = 5.5$ μM) (Santo-Domingo et al., 2007).

While performing short-term experiments with KB-R7943 in an attempt to pharmacologically block NCX in skeletal muscle fibers, we discovered another potent pharmacological activity of the drug: inhibition of excitation-contraction coupling (ECC). ECC in skeletal muscle is a cascade of events that is initiated by the depolarization of T-tubule membrane and activation of dihydropyridine receptor, which is necessary for activation of RyR1, intracellular Ca^{2+} release channels anchored within the sarcoplasmic reticulum (Flucher and Franzini-Armstrong, 1996; Bindokas et al., 2003). Here we show that KB-R7943 interferes with ECC by directly blocking RyR1 and that its inhibitory activity extends to another broadly expressed isoform, RyR2.

Materials and Methods

Materials. KB-R7943, SN-6 (obtained from Tocris Bioscience, Ellisville, MO), and 4-nitrobenzylphenylether (Fig. 1) (obtained from Sigma-Aldrich, St. Louis, MO) were dissolved in dimethyl sulfoxide, giving a stock solution of 50 mM. [^{3}H]Ryanodine ([^{3}H]Ry; 50–60 Ci/mmol) was purchased from PerkinElmer Life and Analytical Sciences (Waltham, MA). The nominal free Ca^{2+} in all basal buffers (before the addition of $CaCl_2$ or EGTA) was measured by Ca^{2+} electrode calibrated to National Bureau of Standards stocks. Free Ca^{2+} concentrations stated in the text were arrived based on the nominal Ca^{2+} plus added $CaCl_2$ and EGTA using the Bound and Determined Software (Brooks and Storey, 1992), which accounts for buffer composition (e.g., ATP), pH, and temperature in calculating the free Ca^{2+}.

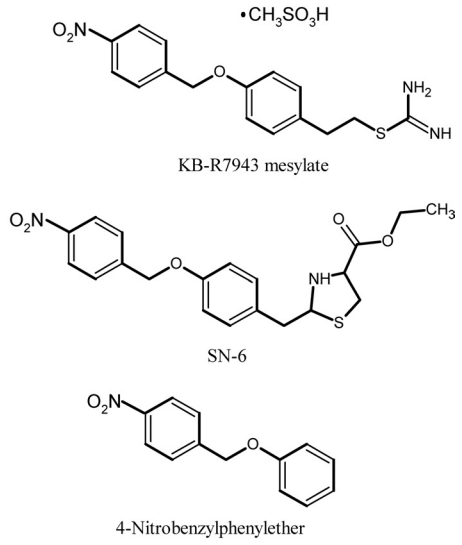

Fig. 1. Chemical structures of the pharmacological agents used in this study.

Preparation of Isolated Fiber Cultures from Adult Mouse Skeletal Muscle. Flexor digitorum brevis (FDB) were dissected from adult mice (C57BL/6), and single intact FDB myofibers were enzymatically isolated as described previously (Brown et al., 2007). After isolation, the fibers were plated on Matrigel-coated plates (BD Biosciences, San Jose, CA) and maintained in Dulbecco's modified Eagle's medium (Invitrogen, Carlsbad, CA) supplemented with 10% bovine serum albumin and 0.1 mg/ml penicillin/streptomycin (Sigma). Fibers were kept overnight in a 5% CO_2 incubator, and experiments were conducted within 12 to 24 h of plating.

Photometric Analysis of Ca^{2+} Transients in Dissociated Fibers. FDB fibers were loaded with Fluo-4 acetoxymethyl ester (10 μM, 40 min) (Invitrogen) in normal Ringer's solution containing 146 mM NaCl, 4.7 mM KCl, 0.6 mM $MgSO_4$, 6 mM glucose, 25 mM HEPES, 2 mM $CaCl_2$, and 0.02% Pluronic F-127 (Invitrogen). The cells were then washed three times with imaging buffer and transferred to the stage of a Nikon Diaphot inverted microscope (Nikon, Tokyo, Japan) and illuminated at 494 nm to excite Fluo-4 with a Delta Ram wavelength-selectable light source (Photon Technology International, Lawrenceville, NJ). Fluorescence emission at 510 nm was captured from individual fibers. Electrical field stimuli were applied using two platinum electrodes fixed to opposite sides of the well and connected to a Master 8 stimulator (A.M.P.I., Jerusalem, Israel) set at a 4-V, 1-ms bipolar pulse duration over a range of frequencies (0.05–20 Hz; 10-s pulse train duration). Fluo-4 fluorescence emission from individual fibers was measured at 200 Hz using digital photometry (model D 104; Photon Technology International).

Ca^{2+} Imaging of HEK 293 Cells. HEK 293 cells stably expressing the $_{wt}$RyR1 ($_{wt}$RyR1-HEK 293) were maintained in Dulbecco's modified Eagle's medium supplemented with 2 mM glutamine, 100 μg/ml streptomycin, 100 U/ml penicillin, 1 mM sodium pyruvate, and 10% fetal bovine serum at 37°C under 5% CO_2 (Pessah et al., 2009). $_{wt}$RyR1-HEK 293 cells were loaded with 5 μM Fluo-4 acetoxymethyl ester at 37°C for 30 min to measure Ca^{2+} transients in an imaging buffer consisting of 140 mM NaCl, 5 mM KCl, 2 mM $MgCl_2$, 2 mM $CaCl_2$, 10 mM HEPES, and 10 mM glucose, pH 7.4, supplemented with 0.05% bovine serum albumin. The cells were washed three times with imaging buffer and additionally incubated for 20 min at room temperature. Dye-loaded cells were washed three times with imaging buffer and imaged with a charge-coupled device camera (model 512B; Photometrics, Tucson, AZ) with a 40× objective lens attached to an IX-71 microscope (Olympus, Center Valley, PA). The sequence of images was captured and monitored using EasyRatioPro (Photon Technologies International, Birmingham, NJ). Caffeine dissolved in the imaging buffer was focally applied for 15 s using AutoMate Scientific (Berkeley, CA). KB-R7943 was dissolved in the imaging buffer, and $_{wt}$RyR1-HEK 293 cells were incubated for 10 min before the application of caffeine.

Preparation of RyR-Enriched Microsomes. Microsomal membrane vesicles (junctional sarcoplasmic reticulum) were prepared as described previously from New Zealand White rabbit (Mack et al., 1992) or C57BL/6J mouse (Buck et al., 1997) skeletal muscle (RyR1) and New Zealand White rabbit and mouse cardiac muscle (RyR2) (Pessah et al., 1990; Zimányi and Pessah, 1991). The preparations were stored in 10% sucrose and 10 mM HEPES, pH 7.4, at −80°C until needed.

[^{3}H]Ry Binding Analysis. [^{3}H]Ry binds with high affinity and specificity to the open state of RyR1 and RyR2 and therefore provides a convenient measure of ligands that influence channel conformation (Pessah et al., 1985, 1987; Zimányi and Pessah, 1991). Microsomal membrane vesicles enriched in RyR1 (50 μg protein/ml) were incubated in the presence or absence of the different NCX inhibitors in a

solution containing 20 mM HEPES, pH 7.1, 140 mM KCl, 15 mM NaCl, 0.1 mM free Ca^{2+}, and 2 nM [^{3}H]Ry. [^{3}H]Ry binding to RyR2 was measured under the same conditions described for RyR1 except that the protein concentration was 0.1 mg/ml. The binding reactions were quenched by filtration through GF/B glass fiber filters and washed twice with ice-cold harvest buffer (20 mM Tris-HCl, 140 mM KCl, 15 mM NaCl, and 0.05 μM $CaCl_2$, pH 7.1). Nonspecific binding was determined by incubating microsomes with 1000-fold excess unlabeled ryanodine. Binding curves were fitted using a nonlinear least-squares regression model with Origin 7.0 software (OriginLab Corp, Northampton, MA) to calculate EC_{50}.

Reconstitution of RyR1 Single Channels in Planar Lipid Bilayer. Single-channel kinetics in bilayer lipid membranes (BLMs) involved reconstitution of RyR1 and RyR2 from skeletal and cardiac SR membranes, respectively, and recording of channel activity was performed as reported previously (Feng et al., 2008). RyR1 channels were reconstituted into planar lipid bilayer [phosphatidylethanolamine/phosphatidylserine/phosphatidylcholine, 5:3:2 (w/w); Avanti Polar Lipids, Inc., Alabaster, AL]. Incorporation of RyR1 channel into BLM was induced by introducing SR vesicles to the *cis* chamber, which had a 10-fold higher Cs^+ concentration relative to the *trans* chamber. The *cis* chamber (virtually grounded) contained 0.8 ml of 500 mM CsCl, a defined concentration of free Ca^{2+} buffered with EGTA (Brooks and Storey, 1992) and 10 mM HEPES, pH 7.4, whereas the *trans* side (voltage input was applied) contained 50 mM CsCl, 0.1 to 3 mM $CaCl_2$, and 10 mM HEPES, pH 7.4. Upon the fusion of SR vesicle into bilayer, *cis* chamber was perfused to prevent more SR fusion. Single-channel activity was measured using a patch-clamp amplifier (Bilayer Clamp BC 525C; Warner Instruments, Hampden, CT) at a holding potential of −40 mV applied to the *trans* chamber. The amplified current signals, filtered at 1 kHz (Low-Pass Bessel Filter 8 Pole; Warner Instruments) were digitized and acquired at a sampling rate of 10 kHz (Digidata 1320A; Molecular Devices, Sunnyvale, CA). All of the recordings were made for at least 2 to 30 min under each experimental condition. The channel open probability (P_o), mean open times, and mean closed-dwell times (t_o and t_c) were calculated without additional filtering by using Clampfit, pClamp software 9.0 (Molecular Devices). KB-R7943 was added to the *cis* chamber (cytoplasmic side of the channel) to test its influence on channel-gating parameters.

Results

KB-R7943 Inhibits Electrically Evoked Ca^{2+} Transients in Adult Skeletal Muscle Fibers. Figure 2A shows a representative record of the Ca^{2+} transients evoked by 0.1-, 5-, or 20-Hz electrical field trains applied to dissociated FDB fibers loaded with Fluo-4. Under these control conditions, the Ca^{2+} transients evoked by electrical pulse trains of 0.1, 5,

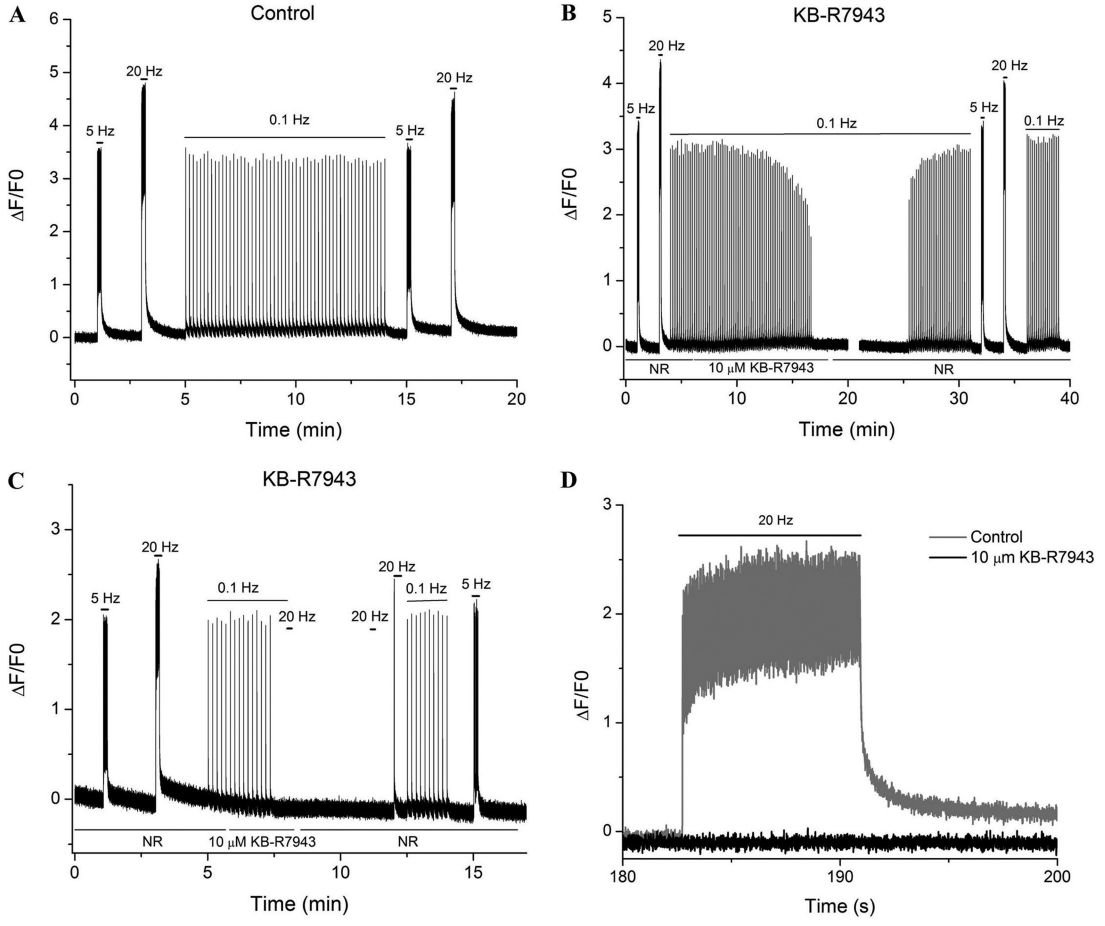

Fig. 2. KB-R7943 inhibits Ca^{2+} transients elicited by low-frequency electrical stimuli in adult dissociated FDB fibers. A, representative Ca^{2+} transient responses in FDB fibers electrically stimulated in the absence of KB-R7943. B, representative Ca^{2+} transients in response to low-frequency electrical stimuli in the presence of 10 μM KB-R7943 in the external perfusion medium. Because of acquisition limitation, our system can acquire the fluorescence in a single file just for 20 min, and the data recording was stopped (gap in the graph) and initiated in another file. C, representative Ca^{2+} transient responses to initial low frequency followed by high-frequency electrical stimuli fibers in the presence of 10 μM KB-R7943. D, expanded time scale of the corresponding section of C, showing superimposed Ca^{2+} traces during 20-Hz electrical pulse train before (gray line) and after (black line) 10 μM KB-R7943. The records shown were taken from continuous measurements of single fibers. Measurements of intracellular Ca^{2+} were acquired at 200 Hz using photometry of individual fibers loaded with Fluo-4, as described under *Materials and Methods*.

and 20 Hz maintained their amplitudes over the entire recording period (Fig. 2A). In our system, low frequency of stimulation (0.1 Hz) evoked short calcium transient lasting less than 300 ms, and these transients recovered to baseline between stimuli. By contrast, higher-frequency stimuli (5 and 20 Hz) evoke Ca^{2+}-transient summation with a sustained increase in cytoplasmic Ca^{2+} that lasted the duration of the stimulus train (Fig. 2A). Electrically evoked Ca^{2+} transients are engaged by bidirectional signaling between $Ca_V1.1$ within the T-tubule membrane and RyR1 in the SR membrane (Nakai et al., 1996), a process termed ECC. In an attempt to study the function of NCX in these fibers, we unexpectedly found that 10 μM KB-R7943 inhibits the Ca^{2+} transients evoked by either 0.1 or 20 Hz stimuli (Fig. 2, B–D). Notice in Fig. 2C and the expanded trace in Fig. 2D that 10 μM KB-R7943 completely inhibited Ca^{2+} transients elicited by a 20-Hz stimulus train in ~30% of the fibers tested. KB-R7943 was also found to inhibit responses to 5-Hz stimuli (data not shown). Within 10 min of drug application, 71% of the fibers paced at 0.1 Hz failed to respond (Fig. 2B; 38 fibers, 11 different isolations) to electrical stimuli. We observed an amplitude decrease (>78% reduction compared with the control period) in 100% of the fibers tested at 20 Hz (20 fibers from 12 different isolations), and the inhibition occurred within 10 min (Fig. 2C). Perfusion of KB-R7943 (10 μM) on fibers stimulated with repetitive 20-Hz pulse trains produced 87.9 ± 4.8% reduction in the integrated peak value measured over a 10-s stimulus train (eight fibers, five different isolations) (Fig. 3A).

A fraction of fibers tested (31.8%) with electrical pulses seemed to be only partially inhibited by KB-R7943 within the time frame of the experiment (Fig. 3, A and B). However, closer inspection of Ca^{2+} transients elicited by 20-Hz pulse trains produced in these apparently "resistant" fibers showed rapid decay in the amplitudes of their Ca^{2+} transients beyond an initial peak, having a duration of only 9.9 ± 12.4 ms (Fig. 3, A and B; n = 14). This is in sharp contrast to fibers perfused in Ringer's solution containing solvent alone, in which Ca^{2+} transients consistently maintained their amplitudes for the duration of the 20-Hz pulse train (Fig. 3, A–C).

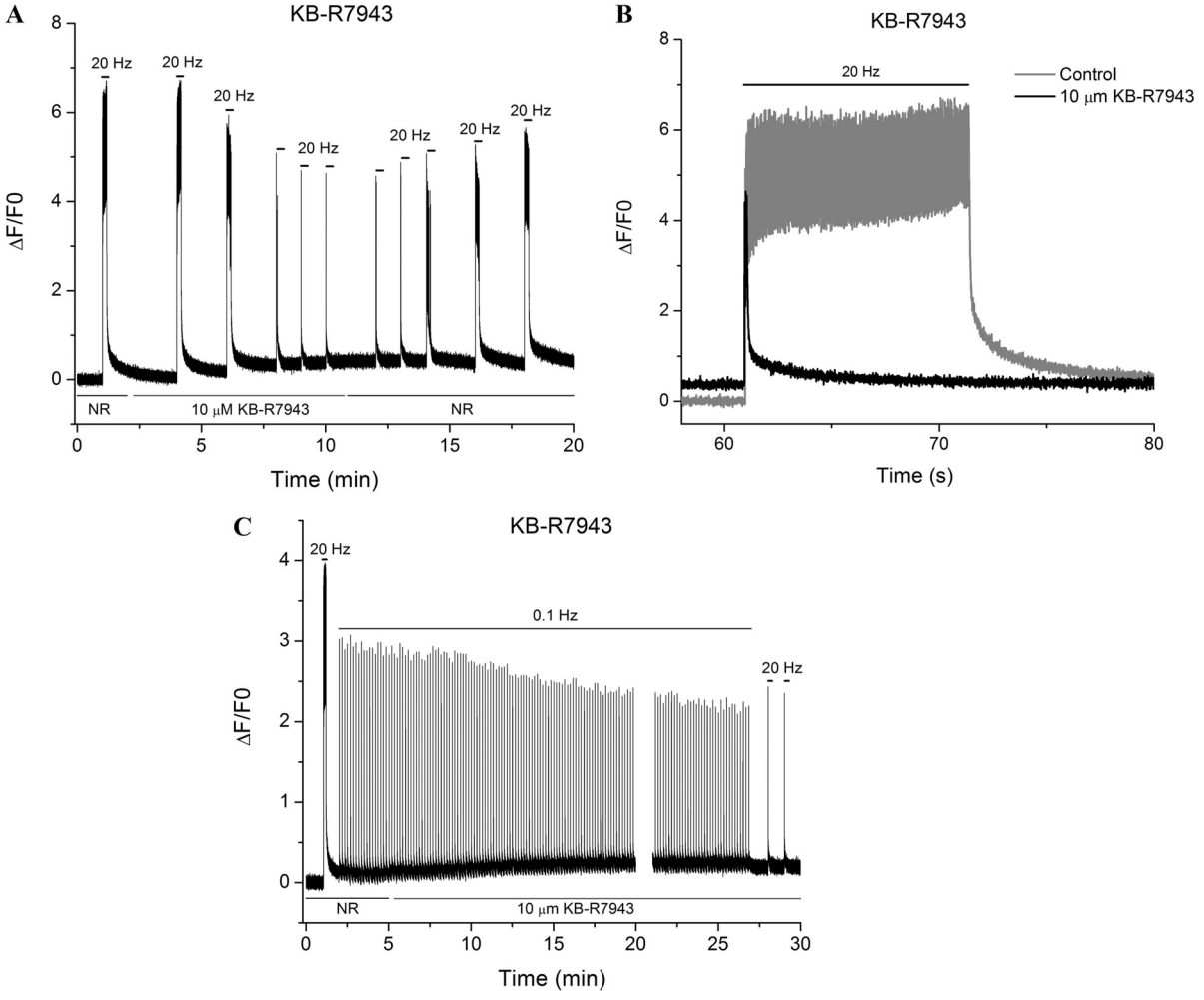

Fig. 3. KB-R7943 inhibits Ca^{2+} transients in fibers stimulated with 20-Hz electrical pulse trains. A, representative Ca^{2+} transients in fibers stimulated with multiple 20-Hz electrical pulse trains lasting 10 s each before and after introducing 10 μM KB-R7943 in the bulk perfusion medium. This experiment was repeated n = 8 times with similar results. B, expanded time scale of the corresponding section of A, showing superimposed Ca^{2+} traces during 20-Hz electrical pulse train before (gray line) and after (black line) 10 μM KB-R7943. C, representative Ca^{2+} transients of resistant fibers stimulated continuously at 0.1 Hz and subsequently with 20-Hz pulse trains (n = 9, five different isolations). The gap in the recording is due to system limitations in acquiring photometry data at high speed for up to 20 min. The gap represents the time needed to initiate a new acquisition file. Measurements of intracellular Ca^{2+} were acquired at 200 Hz using photometry of individual fibers loaded with Fluo-4, as described under *Materials and Methods*.

Those fibers that were resistant to 10 μM KB-R7943 at 0.1 Hz were unable to maintain their normal response to a 20-Hz pulse train (100% of the fibers tested failed; Fig. 3C; $n = 9$, five different isolations).

Inhibition of ECC responses to 0.1- and 20-Hz electrical pulse trains was reversible upon washout with normal Ringer's solution (Fig. 2, B and C, and 3A), and the Ca^{2+} transient amplitudes recovered to pre-exposure levels in all of the cells tested for recovery, regardless of the stimulus frequency ($n = 26$ fibers). Perfusion of 10 μM KB-R7943 in the absence of electrical stimuli produced a negligible influence on Fluo-4 fluorescence in resting fibers (data not shown).

SN-6 is structurally related to KB-R7943 (Fig. 1) and was also shown to block NCX (IC_{50} ~3 μM for NCX1) (Iwamoto, 2004). SN-6 (10 or 20 μM) has no inhibitory effects on the properties of Ca^{2+} transients evoked by either 0.1- or 20-Hz pulse trains (Fig. 4, A and B, respectively; $n = 5$ fibers).

Together, these results suggest that inhibition of ECC by KB-R7943 in electrically stimulated FDB fibers seems to be dependent on the activity of the fiber (i.e., use-dependent). Considering that the block of ECC in KB-R7943-resistant FDB fibers shown in Fig. 3, B and C, occurs rapidly after the initial Ca^{2+} transient suggests that block of the RyR1 occurs once the channel is opened by electrical stimulation. The result shown in Fig. 3C also suggests an activity-dependent (or use-dependent) block, because at low frequency of stimulation (0.1 Hz), KB-R7943 produced modest effects on Ca^{2+}-transient amplitude, whereas the same fiber stimulated at higher frequency (20 Hz) in the presence of the drug was unable to sustain the Ca^{2+} increase. We therefore proceeded to determine whether KB-R7943 interferes with Ca^{2+} release from SR by blocking the open state of RyR1.

KB-R7943 Is a Potent RyR Blocker. Because nanomolar ryanodine preferentially binds to the RyR channels in the open state, the binding of its radiolabeled form [^{3}H]Ry is used to evaluate channel conformation (Pessah et al., 1985, 1987; Zimányi and Pessah, 1991). [^{3}H]Ry binding to mouse skeletal and rabbit cardiac SR preparations enriched in RyR1 and RyR2, respectively, was measured in the presence and absence of KB-R7943 or SN-6. Using assay conditions that promote activation of the respective RyR channel isoforms, KB-R7943 was found to inhibit the high-affinity binding of [^{3}H]Ry in a concentration-dependent manner. The IC_{50} values under the assay conditions used were 5.1 ± 0.9 and 13.4 ± 1.8 μM for mouse RyR1 and RyR2, respectively, and 9.2 ± 0.9 for rabbit RyR1 (Fig. 5, A and B). In contrast, SN-6 (Fig. 5C) and the structurally related compound 4-nitrobenzylphenylether (structure not shown) had negligible inhibitory activity in [^{3}H]Ry binding assays.

KB-R7943 perhaps inhibits the ECC though proteins other than RyR1 (NCX, L-type channels). To test this possibility, we determined whether the drug inhibited RyR1 expressed in HEK 293 cells. These cells do not express any of the known NCX isoforms or RyR1 (Kasir et al., 1999; Hurtado et al., 2006; Pessah et al., 2009). In addition, electrophysiological measurements suggest the absence of endogenous voltage-activated Ca^{2+} currents in these cells (Pérez-García et al., 1995). We assessed the inhibitory effect of KB-R7943 on HEK 293 cells that express wild-type RyR1 ($_{wt}$RyR1) in a stable manner. Cells loaded with Fluo-4 were measured for responses to caffeine using fluorescence-imaging techniques. Figure 6 shows that $_{wt}$RyR1-HEK 293 challenged with caffeine (0.5, 0.75, and 1 mM) respond with a robust Ca^{2+} transient and the amplitude of the Ca^{2+} transient was dependent on the concentration of caffeine (Fig. 6). $_{wt}$RyR1-HEK 293 pretreated with KB-R7943 (10 μM, 10 min) dissolved in the bulk perfusion exhibited significantly attenuated responses to caffeine. In this regard, KB-R7943 produced more pronounced inhibition of caffeine-induced Ca^{2+} release elicited by 1 mM compared with 0.5 and 0.75 mM (60 versus 58 versus 37%, $p < 0.05$, respectively) (Fig. 6, bottom).

The most direct method of determining whether KB-R7943 directly interacts with RyRs to block activity is to measure gating activity of RyR1 or RyR2 channels reconstituted in BLM (Buck et al., 1992). Figure 7A shows that the Ca^{2+}-activated RyR1 single-channel gating transitions were drastically decreased after exposure to 10 μM *cis* (cytoplasmic

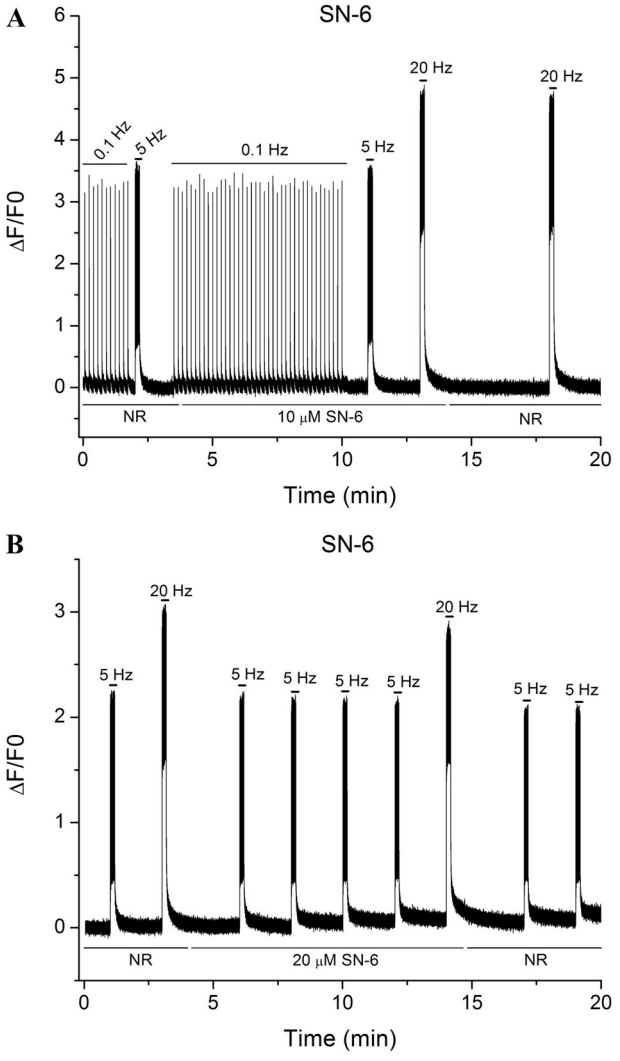

Fig. 4. The NCX inhibitor SN-6 does not inhibit electrically evoked Ca^{2+} transients in FDB fibers. A, a representative response of an FDB fiber stimulated with 0.1- or 20-Hz electrical pulse trains before and after the addition of 10 μM SN-6 to the perfusion medium. The responses shown are representative of $n = 2$ fibers tested in an identical manner. B, representative calcium response in fibers stimulated with repetitive 5 and 20-Hz electrical pulse trains before and after the addition of 20 μM SN-6 in the perfusion medium. These results are representative of $n = 3$ fibers tested in an identical manner. Measurements of intracellular Ca^{2+} were acquired at 200 Hz using photometry of individual fibers loaded with Fluo-4 as described under *Materials and Methods*.

side of the channel) KB-R7943. In the presence of 6 μM free Ca^{2+} in the *cis* solution, the P_o of the channel displayed a typical value of P_o = 0.13, and the current levels associated with the channel-gating events were distributed around the closed (0 current) state (Fig. 7A, right, shows the current amplitude histograms corresponding to the representative current traces). Elevation of *cis* Ca^{2+} to 20 μM activated the channel by increasing P_o 5-fold, increasing the mean open dwell time 3.6-fold and shortening the mean closed time 5.5-fold (higher frequency of current amplitudes distributed near the fully open state; Fig. 7A). Subsequent addition of 10 μM KB-R7943 exerted a significant reduction in the gating frequency of the Ca^{2+}-activated RyR1 channel. The inhibition was reflected in a >11-fold decrease in P_o. The reduced P_o was associated with a 67% decrease in mean open time (τ_o) and a 900% increase in mean closed time (τ_c). In a total of n = 6 independent BLM measurements, 10 μM KB-R7943 inhibited the channel by 82 ± 0.1%. Although KB-R7943-modified RyR1 channels exhibited significantly lower P_o relative to their corresponding control period (measured before drug addition to the *cis* chamber), the drug-modified channels exhibited a burst-like behavior with exceptionally long closed periods compared with control RyR1 channels having similar P_o (Fig. 7A, compare first and third traces). The degree to which KB-R7943 inhibited RyR1 channel gating was further tested with lower free Ca^{2+} concentrations (0.3–1.0 μM) on the cytoplasmic (*cis*) side of the BLM chamber, experimental conditions under which the channel P_o was very low (≤1%). Figure 7B shows approximately 5 min of continuous channel record before and after instillation of 10 μM KB-R7943 in the *cis* chamber. Under these conditions, KB-R7943 produced only a 30% reduction in channel P_o (Fig. 7B).

Similar channel-blocking characteristics of KB-R7943 were observed toward RyR2 channels reconstituted in BLM (Fig. 8). Under activating *cis* Ca^{2+} (1 μM), the RyR2 was engaged in an active gating mode with P_o = 0.76. (Fig. 8A, top current traces and current amplitude histogram). However, after introducing 10 μM KB-R7943 into the *cis* chamber, the RyR2 channel P_o decreased >10-fold (from 0.76 to 0.07). The associated τ_o decreased from 4.39 ± 4.4 to 1.07 ± 1.5 ms, and the τ_c increased from 1.40 ± 1.38 to 14.20 ± 44.7 ms (Fig. 8B). In n = 3 experiments with reconstituted RyR2 channels, 10 μM KB-79743 resulted in 0.92 ± 0.04% reduction of P_o. The KB-R7943-modified RyR2 channel exhibited a burst-like gating behavior similar to that observed with the drug-modified RyR1 channel.

Discussion

Previous work has shown that KB-R7943 can protect cardiac and neuronal cells from calcium overload (Iwamoto et al., 2007; O'Rourke, 2008), the rationale of this approach being the inhibition of the NCX reverse mode that could contribute to calcium overloading within affected cells (Dietz et al., 2007; Wei et al., 2007; Wu et al., 2008). In contrast, NCX activity is believed to protect skeletal muscle from high-frequency fatigue (Sokolow et al., 2004), and KB-R7943 promotes fatigue (Germinario et al., 2008). Our results indicate that functional inhibition of RyR isoforms 1 and 2 in striated muscle may represent a more significant molecular target of KB-R7943 and is likely to be a major contributor to previously reported pharmacological actions of the drug.

[^{3}H]Ry binding and single-channel analyses clearly show that RyR isoforms 1 and 2 are direct targets of KB-R7943 and that the dose range for channel block is within the range for inhibition of NCX. Decrease in RyR activity can provide protection from calcium overload, hence regulating the calcium-mediated cytotoxicity. Considering the pivotal role of RyR in calcium homeostasis (Fill and Copello, 2002; Eisner et al., 2004), a partial inhibition of RyR could per se protect the

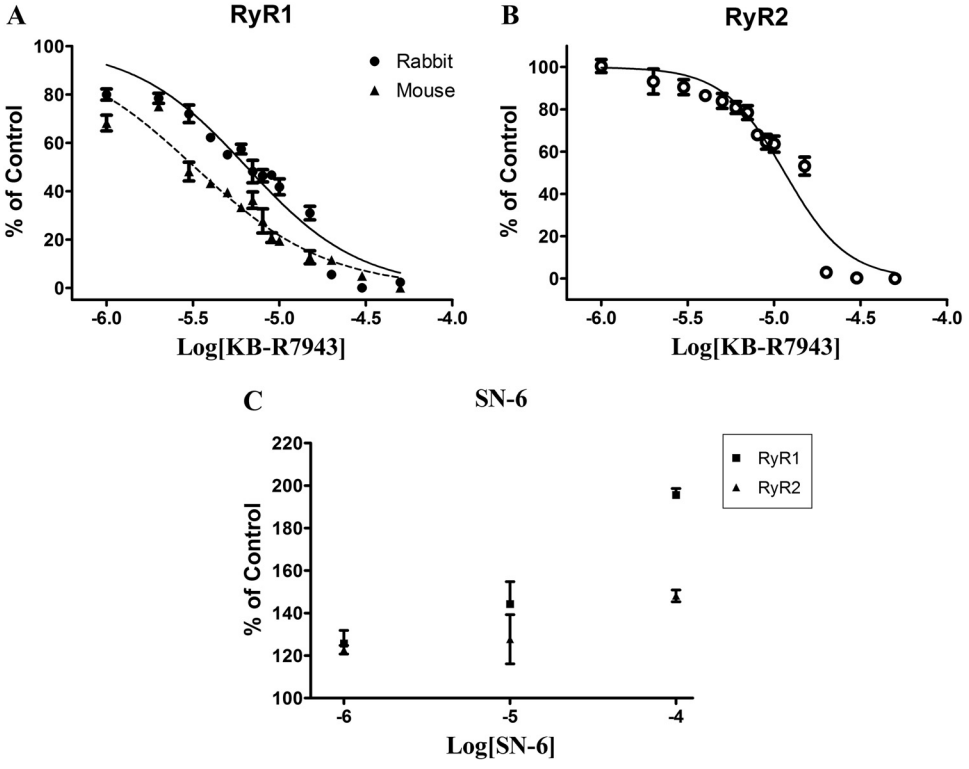

Fig. 5. KB-R7943, but not SN-6, inhibits the binding of [^{3}H]ryanodine to skeletal or cardiac SR membrane fractions. The dose-response of KB-R7943 toward inhibiting [^{3}H]ryanodine ([^{3}H]Ry) binding to rabbit or mouse SR. Inhibition of mouse or rabbit skeletal SR (A) and mouse cardiac SR (B). C, SN-6 fails to inhibit the binding of [^{3}H]Ry to either mouse skeletal (RyR1) or cardiac (RyR2). Inhibition of [^{3}H]Ry binding was normalized to respective control in the absence of drug. The absolute levels of control binding were 0.19 ± 0.04, 0.18 ± 0.09, and 0.29 ± 0.002 for skeletal (mouse), cardiac (mouse), and skeletal (rabbit), respectively. Mean and S.D. data of triplicate experiments are shown. All binding experiments were performed in the presence of 100 μM free Ca^{2+} as described under *Materials and Methods*.

cells from calcium overload. Partial inhibition of RyR2 with flecainide has been shown to prevent catecholaminergic polyventricular tachycardia in mice and humans (Watanabe et al., 2009). Based on experiments in the absence of extracellular Ca^{2+}, Ouardouz et al. (2005) proposed an indirect effect of KB-R7943 on RyR through L-type Ca^{2+} channels. However, binding studies and single-channel records presented here strongly suggest a direct effect of KB-R7943 on RyR. In addition, the KB-R7943 inhibition on caffeine-stimulated Ca^{2+} release in HEK 293 cells stably transfected with RyR1 supports the hypothesis of a direct effect on RyR. Because HEK 293 cells do not express $Ca_v1.2$ protein (Berjukow et al., 1996), an indirect effect of KB-R7943 on RyR mediated by CaV1.2 does not seem to be essential. However, we cannot rule out an additional effect of this inhibitor on dihydropyridine receptor voltage sensor activity.

In our experiments with FDB fibers, inhibition occurred most strongly at high frequencies of stimulation. In 29% of the fibers, we did not observe inhibition at low-frequency stimulation (0.1 Hz, 10 μM KB-R7943); however, at 20 Hz, 100% of fibers tested were inhibited at the same KB-R7943 concentration. Those fibers resistant to inhibition by KB-R7943 when initially stimulated at low frequency failed to maintain the amplitude of their Ca^{2+} transients within milliseconds of initiating a 20-Hz stimulus train. These results suggest that block of RyR1 by KB-R7943 is use-dependent. It is well known that ryanodine binding to RyR is enhanced by conditions that increase RyR activity (Pessah et al., 1987), and electrical stimulation activates ECC by promoting RyR open probability. If KB-R7943 binds preferably to RyR in the open state, this could explain why high-frequency stimuli increase its efficacy as a blocker of ECC. This hypothesis is supported by the fact that a fraction of the KB-R7943 fibers responded with an initial Ca^{2+} peak, which rapidly failed

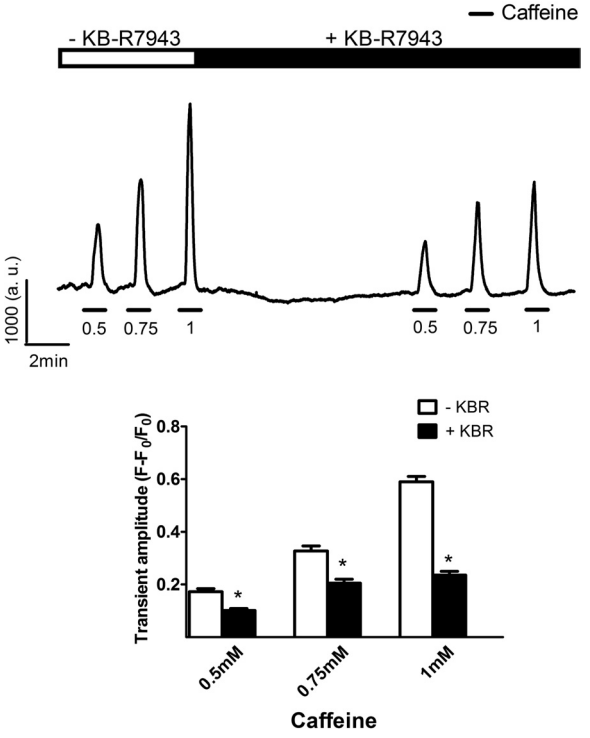

Fig. 6. KB-R7943 inhibits caffeine responses in RyR1-expressing HEK 293 cells. A, focal (15-s) application of caffeine produced Ca^{2+} transients in Fluo-4 loaded HEK 293 cells that stably express RyR1. After the test responses to caffeine in control medium, the cells were incubated with KB-R7963 (10 μM, 10 min) and tested again. Application of caffeine in the presence of KB-R7943 attenuated amplitude of the caffeine-mediated Ca^{2+} transients. B, summary data of dose-response relationships for caffeine in the absence and presence of KB-R7943. Data represent the dose-response relationships averaged from 25 cells (mean ± S.E.M., $*$, $p < 0.05$).

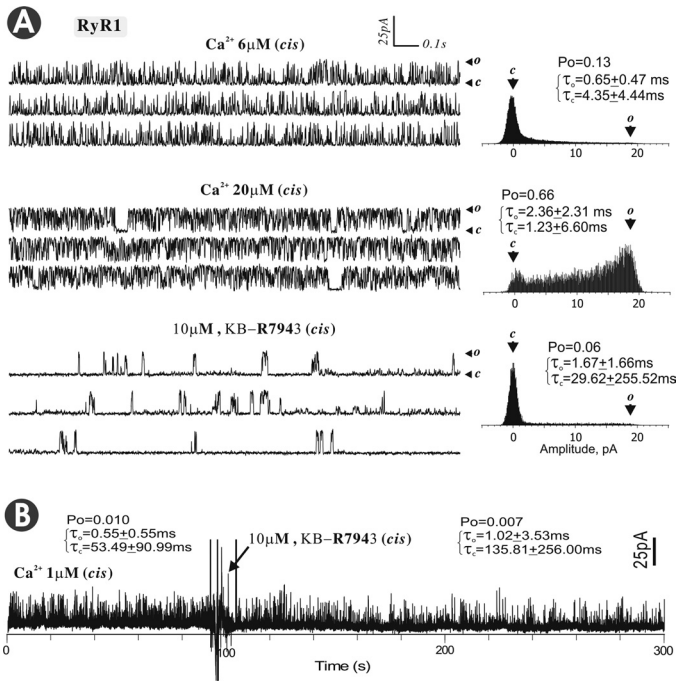

Fig. 7. KB-R7943 inhibits single RyR1 channel activity. Reconstitution of RyR1 single channels was performed by fusing skeletal SR vesicles with BLM as described under *Materials and Methods*. Channel gating was monitored at a holding potential of −40 mV applied to *trans* chamber. A, RyR1 single-channel measurements, the *cis* solution contained 2 mM Na_2ATP and 6 μM Ca^{2+} in the *cis* chamber and 3 mM Ca^{2+} in *trans* chamber. The *cis* Ca^{2+} was stepped to 20 μM Ca^{2+} to enhance channel activity (increase P_o) before the addition of KB-R7943 to the *cis* chamber (traces in A are continuous traces from a single channel). This experiment was repeated on $n = 6$ channels of similar P_o. B, RyR1 channel activity was measured in the presence of suboptimal cytoplasmic/luminal (*cis*/*trans*) conditions (1/100 μM Ca^{2+}) for channel activity before and after adding KB-R7943 (10 μM) to the *cis* chamber. This experiment was repeated with $n = 3$ channels having similar initial P_o (1–3%).

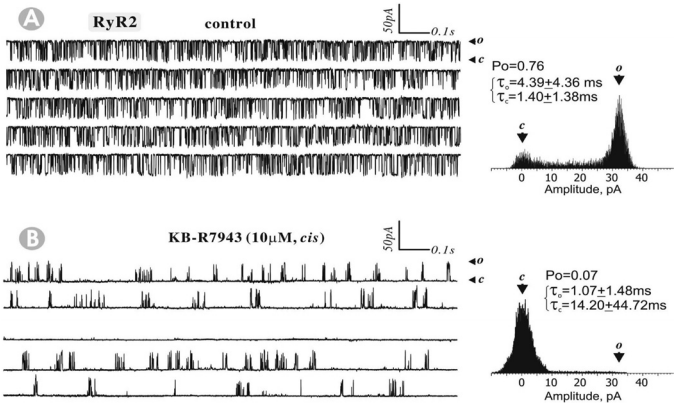

Fig. 8. KB-R7943 inhibits single RyR2 channel activity. RyR2 recordings were made in the presence of 2 mM Na_2ATP, 1 μM *cis* Ca^{2+}, and 100 μM *trans* Ca^{2+}. The current fluctuation is upward for opening, as indicated by an arrow with "O," the maximal current level when channel is fully opened and an arrow with "C" for 0 current level. The P_o, mean open and closed dwell times (τ_o and τ_c, respectively), and the current amplitude histogram were analyzed and are presented.

despite the maintained stimulus train, indicating that RyR1 channel activation precedes complete block. A similar observation was made with analyses of [^{3}H]Ry binding and single-channel experiments. In three channel-reconstitution experiments in which the channel P_o ranged from 1 to 3% (P_o = 0.01–0.03), 10 μM KB-R7943 added to the *cis* chamber reduced P_o by 30 (Fig. 7B) to 200% (data not shown) of control. By contrast, a significantly greater reduction in P_o (>10-fold) was evident when KB-R7943 was introduced to channels gating at higher P_o (Fig. 7A).

Using either approach, conditions that enhance RyR channel activity promote block by KB-R7943. Further evidence of an activity-dependent block can be inferred from results with RyR1-expressing HEK 293 cells, in which inhibition of caffeine-induced Ca^{2+} release was more pronounced at higher caffeine concentrations. However, other factors may also influence the sensitivity of fibers to KB-R7943 block, such as their redox state at the time they were tested, because it is well known that RyR activity is modulated by local redox potential (Feng et al., 2000).

In a recent study using a whole muscle preparation, Germinario et al. (2008) showed that preincubation with 20 μM KB-R7943 for 15 min resulted in an inhibitory effect similar to that observed with a Ca^{2+}-free external solution, and the drug enhanced fatigue. However, altered Ca^{2+} influx or efflux is known to contribute to fatigue (Allen and Westerblad, 2001; Allen et al., 2008). Considering the data presented here, the increased fatigue induced by KB-R7943 is more likely to be due to its ability to inhibit Ca^{2+} release from SR store by directly blocking RyR1 channels. The present results underscore that KB-R7943 at pharmacologically effective concentrations may have multiple targets, and block of RyR channels must be considered in the interpretation of its activity toward muscle physiology. For example, 10 μM KB-R7943 would be expected to have significant influences on both NCX and RyR1. Hence, protection against Ca^{2+} overload may be due to a combination of pharmacological effects. In cardiac muscle, the effect of KB-R7943 has been almost exclusively ascribed to inhibition of NCX activity, the main factor mediating Ca^{2+} extrusion (Lytton, 2007). However, our data suggest that inhibition of RyR2 may significantly contribute to the negative inotropic actions of KB-R7943.

References

Allen DG, Lamb GD, and Westerblad H (2008) Skeletal muscle fatigue: cellular mechanisms. *Physiol Rev* **88:**287–332.

Allen DG and Westerblad H (2001) Role of phosphate and calcium stores in muscle fatigue. *J Physiol* **536:**657–665.

Amran MS, Homma N, and Hashimoto K (2003) Pharmacology of KB-R7943: a Na^+-Ca^{2+} exchange inhibitor. *Cardiovasc Drug Rev* **21:**255–276.

Baczkó I, Giles WR, and Light PE (2003) Resting membrane potential regulates Na^+-Ca^{2+} exchange-mediated Ca^{2+} overload during hypoxia-reoxygenation in rat ventricular myocytes. *J Physiol* **550:**889–898.

Berjukow S, Döring F, Froschmayr M, Grabner M, Glossmann H, and Hering S (1996) Endogenous calcium channels in human embryonic kidney (HEK293) cells. *Br J Pharmacol* **118:**748–754.

Bindokas VP, Kuznetsov A, Sreenan S, Polonsky KS, Roe MW, and Philipson LH (2003) Visualizing superoxide production in normal and diabetic rat islets of Langerhans. *J Biol Chem* **278:**9796–9801.

Blaustein MP and Lederer WJ (1999) Sodium/calcium exchange: its physiological implications. *Physiol Rev* **79:**763–854.

Brooks SP and Storey KB (1992) Bound and determined: a computer program for making buffers of defined ion concentrations. *Anal Biochem* **201:**119–126.

Brown LD, Rodney GG, Hernández-Ochoa E, Ward CW, and Schneider MF (2007) Ca^{2+} sparks and T tubule reorganization in dedifferentiating adult mouse skeletal muscle fibers. *Am J Physiol Cell Physiol* **292:**C1156–C1166.

Buck E, Zimanyi I, Abramson JJ, and Pessah IN (1992) Ryanodine stabilizes multiple conformational states of the skeletal muscle calcium release channel. *J Biol Chem* **267:**23560–23567.

Buck ED, Nguyen HT, Pessah IN, and Allen PD (1997) Dyspedic mouse skeletal muscle expresses major elements of the triadic junction but lacks detectable ryanodine receptor protein and function. *J Biol Chem* **272:**7360–7367.

Dietz RM, Kiedrowski L, and Shuttleworth CW (2007) Contribution of Na^+/Ca^{2+} exchange to excessive Ca^{2+} loading in dendrites and somata of CA1 neurons in acute slice. *Hippocampus* **17:**1049–1059.

Eisner DA, Díaz ME, O'Neill SC, and Trafford AW (2004) Physiological and pathological modulation of ryanodine receptor function in cardiac muscle. *Cell Calcium* **35:**583–589.

Feng W, Liu G, Allen PD, and Pessah IN (2000) Transmembrane redox sensor of ryanodine receptor complex. *J Biol Chem* **275:**35902–35907.

Feng W, Tu J, Pouliquin P, Cabrales E, Shen X, Dulhunty A, Worley PF, Allen PD, and Pessah IN (2008) Dynamic regulation of ryanodine receptor type 1 (RyR1) channel activity by Homer 1. *Cell Calcium* **43:**307–314.

Fill M and Copello JA (2002) Ryanodine receptor calcium release channels. *Physiol Rev* **82:**893–922.

Flucher BE and Franzini-Armstrong C (1996) Formation of junctions involved in excitation-contraction coupling in skeletal and cardiac muscle. *Proc Natl Acad Sci U S A* **93:**8101–8106.

Fraysse B, Rouaud T, Millour M, Fontaine-Pérus J, Gardahaut MF, and Levitsky DO (2001) Expression of the Na^+/Ca^{2+} exchanger in skeletal muscle. *Am J Physiol Cell Physiol* **280:**C146–C154.

Germinario E, Esposito A, Midrio M, Peron S, Palade PT, Betto R, and Danieli-Betto D (2008) High-frequency fatigue of skeletal muscle: role of extracellular Ca^{2+}. *Eur J Appl Physiol* **104:**445–453.

Hurtado C, Prociuk M, Maddaford TG, Dibrov E, Mesaeli N, Hryshko LV, and Pierce GN (2006) Cells expressing unique Na^+/Ca^{2+} exchange (NCX1) splice variants exhibit different susceptibilities to Ca^{2+} overload. *Am J Physiol Heart Circ Physiol* **290:**H2155–H2162.

Iwamoto T (2004) Forefront of Na^+/Ca^{2+} exchanger studies: molecular pharmacology of Na^+/Ca^{2+} exchange inhibitors. *J Pharmacol Sci* **96:**27–32.

Iwamoto T, Watanabe Y, Kita S, and Blaustein MP (2007) Na^+/Ca^{2+} exchange inhibitors: a new class of calcium regulators. *Cardiovasc Hematol Disord Drug Targets* **7:**188–198.

Kasir J, Ren X, Furman I, and Rahamimoff H (1999) Truncation of the C terminus of the rat brain Na^+-Ca^{2+} exchanger RBE-1 (NCX1.4) impairs surface expression of the protein. *J Biol Chem* **274:**24873–24880.

Kraft R (2007) The Na^+/Ca^{2+} exchange inhibitor KB-R7943 potently blocks TRPC channels. *Biochem Biophys Res Commun* **361:**230–236.

Lytton J (2007) Na^+/Ca^{2+} exchangers: three mammalian gene families control Ca^{2+} transport. *Biochem J* **406:**365–382.

MacDonald AC and Howlett SE (2008) Differential effects of the sodium calcium exchange inhibitor, KB-R7943, on ischemia and reperfusion injury in isolated guinea pig ventricular myocytes. *Eur J Pharmacol* **580:**214–223.

Mack WM, Zimányi I, and Pessah IN (1992) Discrimination of multiple binding sites for antagonists of the calcium release channel complex of skeletal and cardiac sarcoplasmic reticulum. *J Pharmacol Exp Ther* **262:**1028–1037.

Matsuda T, Arakawa N, Takuma K, Kishida Y, Kawasaki Y, Sakaue M, Takahashi K, Takahashi T, Suzuki T, Ota T, et al. (2001) SEA0400, a novel and selective inhibitor of the Na^+-Ca^{2+} exchanger, attenuates reperfusion injury in the in vitro and in vivo cerebral ischemic models. *J Pharmacol Exp Ther* **298:**249–256.

Nakai J, Dirksen RT, Nguyen HT, Pessah IN, Beam KG, and Allen PD (1996) Enhanced dihydropyridine receptor channel activity in the presence of ryanodine receptor. *Nature* **380:**72–75.

O'Rourke B (2008) The ins and outs of calcium in heart failure. *Circ Res* **102:**1301–1303.

Ouardouz M, Zamponi GW, Barr W, Kiedrowski L, and Stys PK (2005) Protection of ischemic rat spinal cord white matter: dual action of KB-R7943 on Na^+/Ca^{2+} exchange and L-type Ca^{2+} channels. *Neuropharmacology* **48:**566–575.

Pérez-García MT, Kamp TJ, and Marbán E (1995) Functional properties of cardiac L-type calcium channels transiently expressed in HEK293 cells. Roles of alpha 1 and beta subunits. *J Gen Physiol* **105:**289–305.

Pessah IN, Durie EL, Schiedt MJ, and Zimanyi I (1990) Anthraquinone-sensitized Ca^{2+} release channel from rat cardiac sarcoplasmic reticulum: possible receptor-mediated mechanism of doxorubicin cardiomyopathy. *Mol Pharmacol* **37:**503–514.

Pessah IN, Lehmler HJ, Robertson LW, Perez CF, Cabrales E, Bose DD, and Feng W (2009) Enantiomeric specificity of (−)-2,2′,3,3′,6,6′-hexachlorobiphenyl toward ryanodine receptor types 1 and 2. *Chem Res Toxicol* **22:**201–207.

Pessah IN, Stambuk RA, and Casida JE (1987) Ca^{2+}-activated ryanodine binding: mechanisms of sensitivity and intensity modulation by Mg^{2+}, caffeine, and adenine nucleotides. *Mol Pharmacol* **31:**232–238.

Pessah IN, Waterhouse AL, and Casida JE (1985) The calcium-ryanodine receptor complex of skeletal and cardiac muscle. *Biochem Biophys Res Commun* **128:**449–456.

Pintado AJ, Herrero CJ, García AG, and Montiel C (2000) The novel Na^+/Ca^{2+} exchange inhibitor KB-R7943 also blocks native and expressed neuronal nicotinic receptors. *Br J Pharmacol* **130:**1893–1902.

Santo-Domingo J, Vay L, Hernández-Sanmiguel E, Lobatón CD, Moreno A, Montero M, and Alvarez J (2007) The plasma membrane Na^+/Ca^{2+} exchange inhibitor KB-R7943 is also a potent inhibitor of the mitochondrial Ca^{2+} uniporter. *Br J Pharmacol* **151:**647–654.

Schröder UH, Breder J, Sabelhaus CF, and Reymann KG (1999) The novel Na^+/Ca^{2+} exchange inhibitor KB-R7943 protects CA1 neurons in rat hippocampal slices against hypoxic/hypoglycemic injury. *Neuropharmacology* **38:**319–321.

Seki S, Taniguchi M, Takeda H, Nagai M, Taniguchi I, and Mochizuki S (2002) Inhibition by KB-r7943 of the reverse mode of the Na^+/Ca^{2+} exchanger reduces Ca^{2+} overload in ischemic-reperfused rat hearts. *Circ J* **66:**390–396.

Sokolow S, Manto M, Gailly P, Molgó J, Vandebrouck C, Vanderwinden JM, Herchuelz A, and Schurmans S (2004) Impaired neuromuscular transmission and skeletal muscle fiber necrosis in mice lacking Na/Ca exchanger 3. *J Clin Invest* **113:**265–273.

Stys PK (2004) White matter injury mechanisms. *Curr Mol Med* **4:**113–130.
Stys PK, Waxman SG, and Ransom BR (1992) Ionic mechanisms of anoxic injury in mammalian CNS white matter: role of Na^+ channels and Na^+-Ca^{2+} exchanger. *J Neurosci* **12:**430–439.
Watanabe H, Chopra N, Laver D, Hwang HS, Davies SS, Roach DE, Duff HJ, Roden DM, Wilde AA, and Knollmann BC (2009) Flecainide prevents catecholaminergic polymorphic ventricular tachycardia in mice and humans. *Nat Med* **15:**380–383.
Wei GZ, Zhou JJ, Wang B, Wu F, Bi H, Wang YM, Yi DH, Yu SQ, and Pei JM (2007) Diastolic Ca^{2+} overload caused by Na^+/Ca^{2+} exchanger during the first minutes of reperfusion results in continued myocardial stunning. *Eur J Pharmacol* **572:**1–11.
Wu MP, Kao LS, Liao HT, and Pan CY (2008) Reverse mode Na^+/Ca^{2+} exchangers trigger the release of Ca^{2+} from intracellular Ca^{2+} stores in cultured rat embryonic cortical neurons. *Brain Res* **1201:**41–51.
Zimányi I and Pessah IN (1991) Comparison of [^{3}H]ryanodine receptors and Ca^{++} release from rat cardiac and rabbit skeletal muscle sarcoplasmic reticulum. *J Pharmacol Exp Ther* **256:**938–946.

Address correspondence to: Dr. Isaac N. Pessah, Department of Molecular Biosciences, School of Veterinary Medicine, One Shields Avenue, University of California, Davis, CA 95616. E-mail: inpessah@ucdavis.edu